

MICROSLAB MODEL FOR DIFFUSION-CONTROLLED DRYING OF A FRACTURED POROUS MEDIUM

Randall D. Manteufel, Hannah M. Castellaw, and Stuart A. Stothoff

Center for Nuclear Waste Regulatory Analyses

Southwest Research Institute

6220 Culebra Rd.

San Antonio, TX 78238-5166

(210) 522-5250

FAX: (210) 522-5155

ABSTRACT

An analytic model is developed for diffusion-controlled vapor transfer in a heated, fractured, porous medium. The model is applied to hypothetical, near-field conditions in a high-level waste (HLW) repository that is proposed at Yucca Mountain (YM), Nevada. The model takes into account (i) dry air used to ventilate HLW emplacement drifts, (ii) transient temperatures due to the heat-dissipating nature of nuclear HLW, and (iii) a fractured geologic medium. The model is one-dimensional (1D) and consists of a semi-infinite slab of rock divided into a series of microslabs, across which liquid is assumed not to advect. A heat flux is applied to one boundary, thereby vaporizing the groundwater in the rock. Vapor then diffuses toward the source of heat due to vapor-density gradients between the heated, partially-saturated slab and the dry ventilation air passing through the drift. The model predicts the amount of vapor transferred from the fractured rock to the emplacement drift, and the extent of dryout. The model is compared with the results from a more detailed computer code and found to be acceptably accurate.

NOMENCLATURE

A_i	coefficients for estimating the thermal power for baseline waste description [W/MTIHM]
B_i	coefficients for estimating the thermal power for baseline waste description [1/yr]
D^*	effective vapor diffusion coefficient [6.0×10^{-7} m ² /s]
D^{**}	effective diffusivity for the penetration of the dryout zone [m ² /s]
D	vapor diffusion coefficient in air [2.0×10^{-5} m ² /s]
h	heat of vaporization [2.4×10^6 J/kg]
M_w	molecular weight of water [18.02 kg/kmole]
n	number of microslabs [-]
$P_{v,i}$	vapor pressure of i^{th} microslab [Pa]
$P_{v,0}$	reference vapor pressure [7,380 Pa at 313 K]
q_e'	diffusive heat flux per unit area [W/m ²]
$q_{e,empl}'$	heat flux per unit area at time of emplacement [W/m ²]
Q_{out}'	mass of water leaving the slab per unit area [kg/m ²]
Q_i'	total amount of liquid available for removal per unit area in i^{th} microslab [kg/m ²]
q_v'	diffusive vapor flux per unit area [kg/s · m ²]
$q_{v,i}'$	vapor diffusive flux for the i^{th} microslab [kg/s · m ²]
R	ideal gas constant [8314 J/kmole · K]
S_g	gas saturation (average $S_g=0.5$) [-]
S_i	initial liquid saturation [-]
S_r	residual liquid saturation [-]

NOMENCLATURE (Cont'd)

ΔS	change in liquid saturation [-]
T	temperature [K]
T_0	reference temperature [313 K]
T_i	temperature of the i^{th} microslab [K]
t	time [s]
t_{dry}	total amount of time for the drying process [s]
$\Delta t_{\text{dry},i}$	amount of time for i^{th} microslab to dry [s]
t_{empl}	time from reactor to emplacement [yr]
x	distance [m]
Δx	width of microslabs [m]
α	thermal diffusivity of the rock [m^2/s]
ρ_l	liquid density [kg/m^3]
ρ_v	vapor density [kg/m^3]
$\rho_{v,0}$	vapor density in the emplacement drift [kg/m^3]
$\rho_{v,i}$	vapor density in the i^{th} microslab [kg/m^3]
$\Delta\rho_{v,i}$	change in vapor density from i^{th} microslab to drift [kg/m^3]
τ	tortuosity (2/3) [-]
ϕ	porosity [-]

INTRODUCTION

There are many challenges associated with the safe, long-term isolation of nuclear high-level waste (HLW) from future civilizations and the biosphere. The current approach being pursued in all countries which have nuclear powerplants and the resulting HLW is geologic disposal, which consists of burying the waste deep in the earth (typically hundreds of meters below the ground surface). The site currently being studied in the United States is YM, Nevada which is located on the border of the Nevada Test Site. The site was selected for a number of reasons, including the arid nature of the region (Roseboom, 1983). The current plan consists of tunneling beneath YM and emplacing the waste in a series of mined drifts. The waste is placed in large, thick metal packages which are designed to safely contain the waste for hundreds, and potentially thousands of years. One of the most important aspects which affect waste package lifetime is the thermal-hydrologic environment. Briefly stated, waste packages corrode more rapidly if water is present, and essentially do not corrode if water is absent. Hence, it is important to quantify the thermal-hydrologic environment of the heat-dissipating waste packages in a mined drift.

The thermal-hydrologic environment of waste packages is affected by a number of conditions, including: the amount of downward percolating water, the age and thermal output of the HLW, the density of spacing of waste packages, the hydrologic properties of the geologic material, and the ventilation conditions of the mined excavation. In many studies, the water balance within the mountain is modeled as relatively constant (Pruess et al., 1990a,b; Pruess and Tsang, 1993; Buscheck and Nitao, 1993; Buscheck et al., 1993). It has been recognized that ventilation has the potential of removing significant amounts of heat and groundwater

(Roseboom, 1983; Hopkins et al., 1987; Danko, 1991; Danko and Mousset-Jones, 1992, 1993; Yang and Bhattacharyya, 1994; among others). One recommendation of these works has been to develop a more realistic moisture/vapor transport model to predict rock drying (Danko and Mousset-Jones, 1993). The purpose of this paper is to develop a simple yet realistic model for the drying of the rock under ventilated mine conditions where ventilation removes moisture from the repository.

Fractures can either inhibit or enhance rock dryout. Dryout is enhanced if pressure-driven gas flow occurs in fractures. This was observed in field experiments where fractures were observed to act as preferential pathways for gas flow (Ramirez et al., 1991). The primary cause of pressure-driven gas flow is that the temperature exceeds the boiling temperature. If the temperature remains below the boiling point, then gas flow in fractures will be less significant in enhancing dryout. In laboratory scale experiments, fractures have been observed to inhibit liquid flow (Manteufel et al., 1992). Similarly during isothermal drying and imbibition experiments, microfractures delayed liquid transport from one intact matrix block to the next (Russo and Reda, 1989). It appears the delineation is due to whether the temperatures were significantly high enough to create a pressure-driven flow condition. In low-temperature conditions, the process by which liquid flows in the matrix can significantly reduce the rate of drying, and lead to vapor diffusion being the controlling process.

Similar observations have been reported in the hydrocarbon recovery literature (e.g., Rainwater et al., 1989). Experiments involving forced air vapor extraction of hydrocarbons from the ground have shown that preferential flow paths can develop. The preferential paths develop even in "homogeneous" porous media due to pore-level heterogeneities, and are accentuated by

increasingly larger-scale heterogeneities. The flowing fluid (typically air) develops fingers which act to quickly evaporate the nearby volatiles. However, large stagnant regions can develop between fingers. Concentration gradients are established between the stagnant zones and the flow fingers. The vapors must diffuse to the flow fingers where they are readily removed by advection. The extraction process then becomes controlled by the rate of diffusion of the hydrocarbons from the regions of stagnation to the flow fingers. Models not accounting for preferential flow paths overpredict the amount of hydrocarbon recovery. In the HLW program, the ventilated drifts can be considered as flow fingers and the rock mass as zones of stagnant gas.

The choice of models is important in predicting the drying process in a fractured porous medium. In field heater tests, it was shown that scoping calculations over-predicted the amount of vapor transport near the heater (Ramirez et al., 1989). In another heater test, numerical models (e.g., Pruess et al., 1984) "did not directly predict the small amount of water that entered the [emplacement] hole" where a heater resided (Zimmerman and Blanford, 1986). It is proposed here, that a simple analytic model of diffusion-dominated vapor transfer will aid in more accurately estimating the amount of vapor entering the emplacement drift and the extent of dryout.

One of the challenges of modeling drying is that the rock is fractured and of relatively low hydraulic conductivity. Hence, the liquid is not necessarily advected to the edge of the excavation where it vaporizes. The fracturing and low hydraulic conductivity encourage the vaporization of pore water where it originally resides in the rock. The vapor would then flow by either diffusion (by a vapor density gradient) or advection (by a total gas pressure gradient).

If the temperatures exceed the boiling point, then the pressure-driven gas advection can be significant. If the temperatures remain below the boiling point, then diffusive vapor transport is expected to be dominant. If ventilation is used, then it is possible that the maximum rock temperature will be reduced and remain below the boiling temperature. Based on the cooling effects of ventilation and the presence of a fractured, low hydraulic conductivity medium, the model was developed assuming that drying will be controlled by vapor diffusion.

REPOSITORY LAYOUT

Although a repository layout has not been finalized, a number of conceptual layouts have been discussed. In Figures 1 and 2, a recent repository design is shown for the whole layout and for a single waste package. The design process is ongoing and a final design has not been established. The repository is expected to consist of two large sloping access ramps, two large vertical ventilation shafts, and a series of horizontal emplacement drifts. The emplacement drifts will be located off the main access drift which is connected to the access ramps. The size of the repository remains a design option, as well as the spacing between emplacement drifts and spacing of waste packages inside each drift. Many conceptual designs have a drift diameter of 7.62 m and drift spacing of 20 to 40 m (Saterlie et al., 1994). The waste packages will be introduced into the repository on a rail system using emplacement carts. During the operational life of the repository (~100 yr), the region between the waste package and the rock will probably not be backfilled. This will allow access and periodic inspection of the waste packages to ensure containment of the waste. During this time, it is expected that measures will be available to remediate unfavorable conditions, processes, or events. In order to allow inspection, either continuous or periodic ventilation must be used to cool the areas to be inspected and

4/20

provide oxygen for inspection personnel.

CONCEPTUAL MODEL

It is expected that the repository system will be ventilated using the relatively dry air from arid southern Nevada. The waste packages will be dissipating heat because of the decaying nature of radioactive waste. The surrounding rock will heat up. The higher rock temperature creates a vapor density gradient towards the drift which is assumed to have a continual or periodic supply of cool dry air. The degree of fracturing in the rock has been measured from boreholes and outcrops of the rock unit (Topopah Spring Member of Paintbrush Tuff) where the emplacement drifts are to be located. It has been estimated that the density of fractures range from 10 to 40 per cubic meter with the majority oriented normal to the bedding plain of the rock unit (i.e., vertical fractures) (DOE, 1988). The number of mine excavation-induced fractures is difficult to assess; however, it is assumed that there are a sufficient number of fractures to prohibit liquid flow in the rock matrix.

Figure 3 illustrates the conceptual model. A heat load applied to the drift walls is represented by arrows on the left boundary. The cooling effects of air circulating in the drifts are not modeled directly except to maintain the maximum rock temperature below boiling. Diffusion occurs in the direction of the drift across transversely oriented fractures. The analytic model is 1D in the radial direction from the drift. A finite section of the rock mass is modeled. The right boundary is far from the opening and is assumed to have no flow. The rock heats up causing temperature, vapor-pressure, and vapor-density gradients. The dry air in the drift induces a vapor-density gradient and vapor flow in the direction of the drift. In drying of unfractured, porous media, liquid is frequently assumed to advect to the surface due to suction-

pressure gradients, where it vaporizes and is removed. This model, however, assumes that liquid advection cannot occur across the microfractures. The liquid must vaporize within the microslab of rock and diffuse to the surface, hence moisture transport is solely due to diffusion-controlled vapor transfer. Two cases were considered where the liquid vaporizes on the right side of the microslab and must diffuse through it to reach the surface (case 1), or liquid vaporizes on the left side of the microslab (case 2). The true solution lies between these two cases. In either case, microslabs do not begin to dry until the adjacent microslab is dry. Fracture density is simulated by varying the number of microslabs.

MATHEMATICAL THEORY

Heat Transfer

In this section, the equations used to predict the evolving temperature and vapor density fields are discussed (the symbols are defined in the list of nomenclature). The time-variant temperature distribution is based on the heat conduction equation (where the vaporization of *in situ* groundwater is negligible for the low porosity, high thermal conductivity rock of interest).

$$\frac{\partial T}{\partial t} = \alpha \frac{\partial^2 T}{\partial x^2}$$

The heat flux for decaying HLW is expressed as a sum of exponentials, which is a good approximation for up to 1,000 yr (DOE, 1993).

$$q_e'' = \sum_{i=1}^4 A_i^* e^{-B_i t}$$

The scaling coefficients are related to the age of the waste, t_{empl} , and the density of waste packages.

$$A_i^* = \frac{Q_{e, emp1} A_i e^{-B_i \cdot t_{emp1}}}{\sum_{i=1}^4 A_i e^{-B_i \cdot t_{emp1}}}$$

The A and B coefficients are from U.S. Department of Energy (DOE) YM Reference Information Base (DOE, 1993) and are listed in Table 1. These equations capture the time-varying nature of the waste. The spatial and temporal temperature distribution is calculated so that the vapor pressure can be calculated using Claperyon's equation (Wark, 1983).

$$P_{v, i} = P_{v, 0} \exp\left(\frac{hM_w}{R} \left(\frac{1}{T_0} - \frac{1}{T_i}\right)\right)$$

The vapor density is calculated using the ideal gas law.

$$\rho_{v, i} = \frac{P_{v, i} M_w}{RT_i}$$

The vapor density is required to compute the vapor transfer.

Vapor Transfer

Vapor diffusion is governed by the conservation of species equation where the only transport mechanism is assumed to be diffusion.

$$\frac{\partial}{\partial t} (\phi S_g \rho_v) = \frac{\partial}{\partial x} \left(D^* \frac{\partial \rho_v}{\partial x} \right)$$

The effective vapor diffusion coefficient in a partially saturated porous medium, D^* , is related to the vapor diffusion coefficient in still air.

$$D^* = \tau \phi S_g D$$

The accumulation of vapor at a point is negligible in comparison with the flow of vapor. Hence,

the conservation equation reduces to a statement that the diffusive flux is constant from the microslab where it is generated to the boundary where it is removed

$$q_v'' = -D \cdot \frac{d\rho_v}{dx}$$

The mass of water leaving the slab is the time integral of the transient diffusion vapor flux at the slab boundary.

$$Q_{out}'' = \int q_v'' dt$$

In the model each microslab dries successively, where the second microslab does not dry until the first is completely dry. The diffusive vapor flux for each microslab (per unit area) is based on an approximation of Fick's law,

$$q_{v,i}'' = D \cdot \frac{\Delta \rho_{v,i}}{i \Delta x}$$

where i is the i^{th} microslab from the boundary. The change in vapor density from the i^{th} microslab to the boundary is

$$\Delta \rho_{v,i} = \rho_{v,i} - \rho_{v,0}$$

The vapor density at the boundary, $\rho_{v,0}$ is approximated to be 0.015 kg/m^3 , corresponding roughly to a temperature of $25 \text{ }^\circ\text{C}$ and a relative humidity of 65 percent. The total amount of water available for removal (per unit area) in each microslab is the same (because each slab is of equal thickness) and is given by:

$$Q_i'' = \Delta S \phi \rho_l \Delta x$$

where the saturation available for removal is related to the initial and residual saturations

$$\Delta S = S_i - S_r$$

The rate of vapor removal is constant for each microslab because the effects of vapor pressure lowering are important only at low saturations (i.e., high suction pressures), and the vapor density at the boundary is assumed constant. The time for one microslab to dry is related to the rate of drying and the total water available for removal.

$$Q_i'' = q_{v,i}'' \cdot \Delta t_{dry,i}$$

which leads to:

$$\Delta t_{dry,i} = \frac{\Delta S \phi \rho_l i (\Delta x)^2}{D^* \Delta \rho_{v,i}}$$

The total amount of time required for the entire slab to dry is the sum of all microslab drying times,

$$t_{dry} = \sum_{i=1}^n \frac{\Delta S \phi \rho_l i (\Delta x)^2}{D^* \Delta \rho_{v,i}}$$

where n is the total number of dry microslabs. The time required to dry a given thickness of rock can be calculated using these results.

The above relationships were used to numerically predict the rate and extent of dryout. In addition, the results can be approximated further to yield simple scaling relationships for the rate of dryout and cumulative amount of liquid removed.

The drying process behaves as if a volatilization front were passing through the medium.

The penetration depth of the front is

$$L_{dry} = \sum_{i=1}^n \Delta x$$

which can be expressed as

$$\Delta x = \frac{L_{dry}}{n}$$

Although $\Delta \rho_{v,i}$ is a function of time and location (i.e., i), it is approximated with an appropriate mean so that the drying time can be related to the extent of dryout

$$t_{dry} = \frac{\Delta S \phi \rho_l (L_{dry})^2}{D^* \Delta \bar{\rho}_v} \sum_{i=1}^n \frac{i}{n}$$

It is noted that

$$\sum_{i=1}^n \frac{i}{n} = \frac{n+1}{2}$$

which for large n is approximately $n/2$. Hence, the familiar diffusion result has been derived that the penetration depth of the dryout zone is proportional to the square root of time

$$L_{dry} = \sqrt{D^{**} t_{dry}} \sim \sqrt{t_{dry}}$$

where an effective diffusivity for the penetration of the volatization front is

$$D^{**} = \frac{2D^* \Delta \bar{\rho}_v}{\Delta S \phi \rho_l}$$

$$\Delta \bar{\rho}_v \doteq \rho_v [T(x=0, t=t_{dry})] - \rho_{v,0}$$

This approximation has been found to yield accurate estimates of the dryout depth. The cumulative amount of liquid removed is related to the dryout penetration depth so that it also scales as the square root of time

$$Q''_{out} = \phi \Delta S L_d \sim \sqrt{t_{dry}}$$

These scaling results were found to be consistent with the more accurate numerical results presented in the next section.

RESULTS

To simulate nonisothermal transient heat conditions, it was first necessary to calculate the heat flux. Figure 4 illustrates the area-averaged decay heat flux applied at the boundary (which is the surface of the mined drift). The integral of heat flux is shown along the right axis and indicates the total amount of energy input into the system per unit area over time. The transient temperature distribution was then calculated.

Figure 5 illustrates the spatial and temporal temperature distribution in the rock slab for the conditions shown. The temperature does not exceed the boiling point of water for the time period based on the heat load simulated. The initial heat flux on the drift wall is 11.0 W/m^2 . This flux corresponds to a 14 W/m^2 areal power density with 8 m diameter drifts at a 20 m drift spacing. This is roughly equivalent to the reference case thermal load of 14.7 W/m^2 (Saterlie and Thomson, 1994). This does not account for heat removed by ventilation. The maximum temperature in the simulation peaked at about $95 \text{ }^\circ\text{C}$ near 40 yr. It is recognized that zones of rock will attain higher than boiling temperatures and it is suggested that more detailed models be employed, accounting for more realistic geometries (discrete heat sources located in parallel drifts versus a uniform flux into a semi-infinite region) and accounting for the removal of heat

by ventilation. The heat load was selected so that it roughly corresponds to the reference case thermal load, yet the maximum temperature never exceeds the boiling temperature.

The cumulative mass of vapor extracted under nonisothermal, transient heat conditions is shown in Figure 6. For the conditions stated, 220 kg/m² of vapor is removed. This corresponds to drying about 2.8 m of the rock slab. The rate of vapor extraction is higher at early times and gradually decreases over the 50-yr simulation period down to about 5 kg/m² per yr. The first meter of rock dries in about 15 yr.

Figure 7 shows the saturation of each microslab over time in the 5-microslab case shown in Figure 6. Each microslab corresponds to a distance of 1 m. The initial saturation was set at 0.9 and a residual saturation of 0.1 was assumed. When the residual saturation was reached the microslab was considered dry. The slopes of the lines representing slabs 1, 2, and 3 are decreasing, illustrating that the rate of dryout decreases over time. This is due to lower vapor-density gradients which are influenced most strongly by the increasing lengths of flow paths moving away from the surface.

The method and results presented here are compared with results generated by a computer code developed by Stothoff (1994). The code models the coupled 1D transport of energy and moisture in a porous medium. Two cases were investigated: a direct analog of the analytic solution method, where moisture flows only by vapor diffusion; and an analog in which no fractures are present and liquid flow can occur in the rock matrix. In the second analog, the matrix flow properties are taken from Flint and Flint (1994), representing welded Topopah Spring tuff [saturated hydraulic conductivity is 5.9×10^{-11} m/s and relative permeability is represented by van Genuchten (1980) functions with an n parameter of 1.45 and an alpha

parameter of 0.210 m^{-1}]. In both cases, the numerical model extends to 50 m (far beyond the influence of the ventilation) and is discretized with 500 elements evenly grading from 0.01 m at the drift wall to 0.37 m at the outer boundary. Ventilation is modeled by imposing ($\rho_{v,o}$) at a distance 0.1 m into the drift and allowing diffusion from the porous medium with the vapor diffusion constant in still air.

In Figure 8, the vapor density profiles are plotted for the two cases. The top figure is for the case without liquid advection and the bottom includes liquid advection. A distinct peak in the vapor pressure is observable. The location and magnitude of the peak varies with time. The peak is an indication of a narrow zone of vaporization of the groundwater. The location of the peak is an indication of the extent of rock dryout. To the left of the peak (towards the drift), the vapor density profile is very uniform. This indicates a constant vapor mass flux from the peak to the ventilated boundary. Only minor differences exist between the two cases so that liquid advection is noted not to have a strong effect on vapor flow. The numerical predictions support the approximation in the microslab model that the microslabs dry sequentially.

In Figure 9, the liquid saturation profiles for the two cases are plotted. The top figure is for the case without liquid advection and the bottom includes liquid advection. In both cases, a large change in the saturation is restricted to a relatively narrow spatial zone. This confirms the observation that the dryout zone develops as if a front were propagating through the medium. The case with liquid advection produced a more gradual transition in saturation to the right of the dryout zone. This more gradual transition leads to liquid flow toward the vaporization region. Both cases produce similar saturation profiles to the left of the vaporization region, indicating that advection does not affect this region. Both cases predict nearly the same extent

of dryout (3.8 m at 50 yr) indicating that advection affects the saturation profile, but not the overall drying process.

In Figure 10, the rate of removal and cumulative removal of liquid water are plotted for both cases. The case with liquid advection yields larger rates of removal and amounts of cumulative liquid mass removed. At early times ($t < 5$ yr), the rate of drying is much larger than at longer times, and at $t=0$ the rate of drying is theoretically infinite. At early times, the difference between the rates of removal for the two cases is most significant, indicating that liquid advection enhances drying. The difference become increasingly smaller at longer times, indicating that vapor diffusion more strongly limits the overall drying process. The cumulative removal is the time integral of the rate of removal, and the difference between the two cases increases with time. The cumulative removal predicted by the computer code supports the microslab model predictions (compare Figures 6 and 10).

The method and results presented here were compared with other published works. Hopkins et al. (1987) describe 1D and two-dimensional (2D) isothermal studies where liquid was assumed to advect in the rock matrix towards the drift wall, and then be removed by the ventilation air. Because their model was isothermal, vapor diffusion was negligible in comparison with liquid advection and it was neglected in their model. As such, the dominant mechanism for transport is different than in this work, and a quantitative comparison is impossible. However, qualitatively the results were found to be similar in that approximately 2 to 5 m of rock dried during 50 yr of continuous ventilation.

Danko and Mousset-Jones (1993) have reported numerical predictions of heat and moisture transport in a ventilated drift with heat-dissipating HLW. The moisture removal model

is based on a wall wetness ratio which is discussed in the mine ventilation literature (Chang and Greuer, 1985; Laage et al., 1994). They conclude that relatively low values of airflow can result in high values of groundwater removal. Their calculations show that "there is a potential that a total amount of 0.72 metric tons of water per linear meter of drift per year can be permanently removed from the repository horizon." This corresponds to approximately a five times higher rate of drying than reported in this paper. They note, however, that the reported potential for water removal needs to be checked against the availability of water migrating towards the drift, and the wall wetness ratio needs to be adjusted using a coupled hydrothermal model. It is proposed that the model developed in this paper can be incorporated into an effective wall wetness ratio, however this is beyond the scope of this paper.

Implications of this work are that ventilation may produce a zone of dry rock surrounding the emplacement drifts. This zone may have the beneficial aspects of yielding a lower rate of liquid transport towards the HLW, and a lower rate of aqueous transport of radionuclides into the geologic medium. These results, however, are sensitive to the conceptual model. In this paper, we assumed the dryout was controlled by vapor diffusion. An alternative conceptual model has been described in the literature (e.g., Hopkins et al., 1987) which assumes the process is controlled by liquid advection in the rock matrix. Alternatively, one may hypothesize the process is controlled by a few sparse flowing fractures (e.g., the weeps flow model discussed by Gauthier et al, 1992). In each model, important assumptions are made and values chosen for key parameters. Different models can be used to predict the effects of ventilation before the repository is constructed. After the mine is constructed, however, the actual performance can be monitored relatively easily based on measurements of values such as wet/dry bulb

temperature and air flow rates. Models then can be calibrated to the actual conditions.

CONCLUSIONS

The microslab model of diffusion-dominated drying of heated, fractured rock provides:

1. Means for quick calculations to determine the amount of vapor extracted from rock surrounding a source of radioactive decay heat and the extent of rock dryout
2. Means for quick calculations which can be used to check the results of more elaborate computer predictions
3. Insights into scaling the rate and extend of rock dryout ($Q_{out}'' \sim L_{dry} \sim \sqrt{t_{dry}}$)

For conditions relevant to YM over a 50 yr simulation period, the model shows:

1. The rate of dryout varies from 10 to 5 kg/m² per year, decreasing with time
2. Approximately 220 to 320 kg/m² of vapor is extracted from the rock
3. The extent of dryout into the rock from the drift wall is about 3 to 4 m

ACKNOWLEDGEMENTS

This paper was prepared to document work performed by the Center for Nuclear Waste Regulatory Analyses (CNWRA) for the U.S. Nuclear Waste Regulatory Commission (NRC) under Contract No. NRC-02-93-005. The activities reported herein were performed on behalf of the NRC Office of Nuclear Regulatory Research, Division of Regulatory Applications. The report is an independent product of the CNWRA and does not necessarily reflect the views or regulatory position of the NRC.

REFERENCES

Buscheck, T.A., and Nitao, J.J., 1993, "Repository-Heat-Driven Hydrothermal Flow at Yucca Mountain, Part I: Modeling and Analysis," *Nuclear Technology*, Vol. 104, pp. 418-448.

- Buscheck, T.A., Nitao, J.J., and Wilder, D.G., 1993, "Repository-Heat-Driven Hydrothermal Flow at Yucca Mountain, Part II: Large-Scale In Situ Heater Tests," *Nuclear Technology*, Vol. 104, pp. 449-471.
- Chang, X., and Greuer, R.E., 1985, "Simplified Method to Calculate the Heat Transfer Between Mine Air and Mine Rock," *2nd US Mine Ventilation Symposium*, P. Mousset-Jones, ed., A.A. Balkema, Accord, MA, pp. 429-438.
- Danko, G., 1991, "Emplacement Rift Temperature Reduction by Cooling Enhancement and Ventilation," *Proceedings of the Second Annual International Conference on High-Level Radioactive Waste Management*, American Nuclear Society, La Grange Park, IL, pp. 1,585-1,593.
- Danko, G., and Mousset-Jones, P., 1992, "Coupled Heat and Moisture Transport Model for Underground Climate Prediction," *Proceedings of the 3rd International Conference on High-Level Radioactive Waste Management*, American Nuclear Society, La Grange Park, IL, pp. 790-798.
- Danko, G., and Mousset-Jones, P., 1993, "Modeling of the Ventilation for Emplacement Drift Re-Entry and Rock Drying," *Proceedings of the International High-Level Radioactive Waste Management Conference*, American Nuclear Society, La Grange Park, IL, pp. 590-599.
- DOE (U.S. Department of Energy), 1988, "Site Characterization Plan: Yucca Mountain Site, Nevada Research and Development Area, Nevada," DOE/RW-0199, DOE, Washington D.C.
- DOE (U.S. Department of Energy), 1993, "Yucca Mountain Project Reference Information

- Base," YMP/93-02, Rev.3. DOE, Las Vegas, NV.
- DOE (U.S. Department of Energy), 1994, *Yucca Mountain Site Characterization Project Technical Program Review*, DOE, Las Vegas, NV.
- Flint, A.L., and L.E. Flint, 1994, Spatial Distribution of Potential Near Surface Moisture Flux at Yucca Mountain, Proceedings of the International High-Level Radioactive Waste Management Conference, American Nuclear Society, La Grange Park, IL, pp. 2,352-2,358.
- Gauthier, J.H., Wilson, M.L., Peters, R.R., Dudley, A.L., and Skinner, L.H., 1992, *Total System Performance Assessment Code (TOSAPAC) Volume 2: User's Guide SAND85-0004*, Sandia National Laboratories, Albuquerque, NM.
- Hopkins, P.L., Eaton, R.R., and Sinnock, S., 1987, "Effect of Drift Ventilation on Repository Hydrology and Resulting Solute Transport Implications," *Flow and Transport Through Unsaturated Fractured Rock*, D.D. Evans and T.J. Nicholson, eds., Geophysical Monograph 42, American Geophysical Union, Washington, D.C., pp. 177-183.
- Laage, L., Yang H., Greur R., and Pomroy W., 1994, "Recent Improvements in the MFIRE Ventilation and Fire Simulator," *Mining Engineering*, February, pp. 145-148.
- Manteufel, R.D., Green, R.T., Dodge, F.T., Svedeman, S.J., 1992, "An Experimental Investigation of Two-Phase Two Component Nonisothermal Flow in a Porous Medium with a Simulated Fracture," *Heat and Mass Transfer in Porous Media*, I. Catton, ed., American Society of Mechanical Engineers, New York, NY, HTD-Vol. 216, pp. 9-18.
- Pruess, K., Tsang, Y.W., and Wang, J.S.Y., 1984, "Numerical Studies of Fluid and Heat Flow Near High-Level Nuclear Waste Packages Emplaced in Partially Saturated Fractured

- Tuff," LBL-18552, Lawrence Berkeley Laboratory, University of California, Berkeley, CA.
- Pruess, K., Wang, J.S.Y., and Tsang, Y.W., 1990a, "On Thermohydrologic Conditions Near High-Level Nuclear Wastes Emplaced in Partially Saturated Fractured Tuff 1. Simulation Studies with Explicit Consideration of Fracture Effects," *Water Resources Research*, Vol. 26(6), pp. 1,235-1,248.
- Pruess, K., Wang, J.S.Y., and Tsang, Y.W., 1990b, "On Thermohydrologic Conditions Near High-Level Nuclear Wastes Emplaced in Partially Saturated Fractured Tuff 2. Effective Continuum Approximation," *Water Resources Research*, Vol. 26(6), pp. 1,249-1,261.
- Pruess, K. and Tsang, Y., 1993, "Modeling of Strongly Heat-Driven Flow Processes at a Potential High-Level Nuclear Waste Repository at Yucca Mountain, Nevada," *Proceedings of the Fourth Annual International Conference on High-Level Radioactive Waste Management*, American Nuclear Society, La Grange Park, IL, pp. 568-575.
- Rainwater, K., Zaman, M.R., Claborn, B.J., Parker, H.W., 1989, "Experimental and Modeling Studies of In Situ Volatilization: Vapor-Liquid Equilibrium or Diffusion-Controlled Process?," *Proceedings of the NWWA/API Petroleum Hydrocarbons Conference*, Houston, TX, pp. 457-472.
- Ramirez, A.L., et al., 1989, "Prototype Engineered Barrier System Field Tests-Progress Report," *Proceedings of the Topical Meeting on Nuclear Waste Isolation in the Unsaturated Zone Focus '89*, American Nuclear Society, La Grange Park, IL, pp. 30-37.
- Ramirez, A.L. (ed.), 1991, "Prototype Engineered Barrier System Field Test (PEBSFT) Final Report," UCRL-ID-106159, Lawrence Livermore National Laboratory, Livermore, CA.

- Roseboom, E.H., 1983, "Disposal of High-Level Nuclear Waste Above the Water Table in Arid Regions," Geological Survey Circular 903. U.S. Geological Survey, Alexandria, VA.
- Russo, A.J., and Reda, D.C., 1989, "Drying of an Initially Saturated Fractured Volcanic Tuff," *Journal of Fluids Engineering*, Vol. 111, pp. 191-196.
- Saterlie, S.F., and B.H. Thomson. 1994. "FY93 Thermal Loading Systems Study Final Report." B00000000-01717-5705-00013. Washington, DC: DOE Office of Civilian Radioactive Waste Management.
- Stothoff, S., 1994, BREATH Version 1.0-Coupled Flow and Energy Transport in Porous Media, CNWRA 94-020, San Antonio, TX: Center for Nuclear Waste Regulatory Analyses.
- van Genuchten, M.Th., 1980, A Closed-Form Equation for Predicting the Hydraulic Conductivity of Unsaturated Soils, *Soil Science Society of America Journal* 44, pp. 892-898.
- Wark, K., 1983, *Thermodynamics*. New York, NY: McGraw-Hill.
- Yang, H. and Bhattacharyya, K.K., 1994, "Ventilation Considerations for Repository Subsurface Advanced Conceptual Design," *Proceedings of the International High-Level Radioactive Waste Management Conference*, American Nuclear Society, La Grange Park, IL, pp. 530-537.
- Zimmerman R.M., and Blanford, M.L., 1986, "Expected Thermal and Hydrothermal Environments for Waste Emplacement Holes Based on G-tunnel Heater Experiments," *27th U.S. Symposium on Rock Mechanics*, H. Hartman, ed., Society of Mining Engineers, Inc., Littleton, CO, pp. 874-882.

14/20

Table 1. Coefficients in HLW Heat Source (DOE, 1993)

i	A [W/MTIHM]	B [Yr ⁻¹]
1	1.665×10^2	1.106×10^{-3}
2	4.086×10^2	1.346×10^{-2}
3	7.873×10^2	3.130×10^{-2}
4	7.201×10^3	4.437×10^{-1}

NOTE: MTIHM = Metric Ton of Initial Heavy Metal

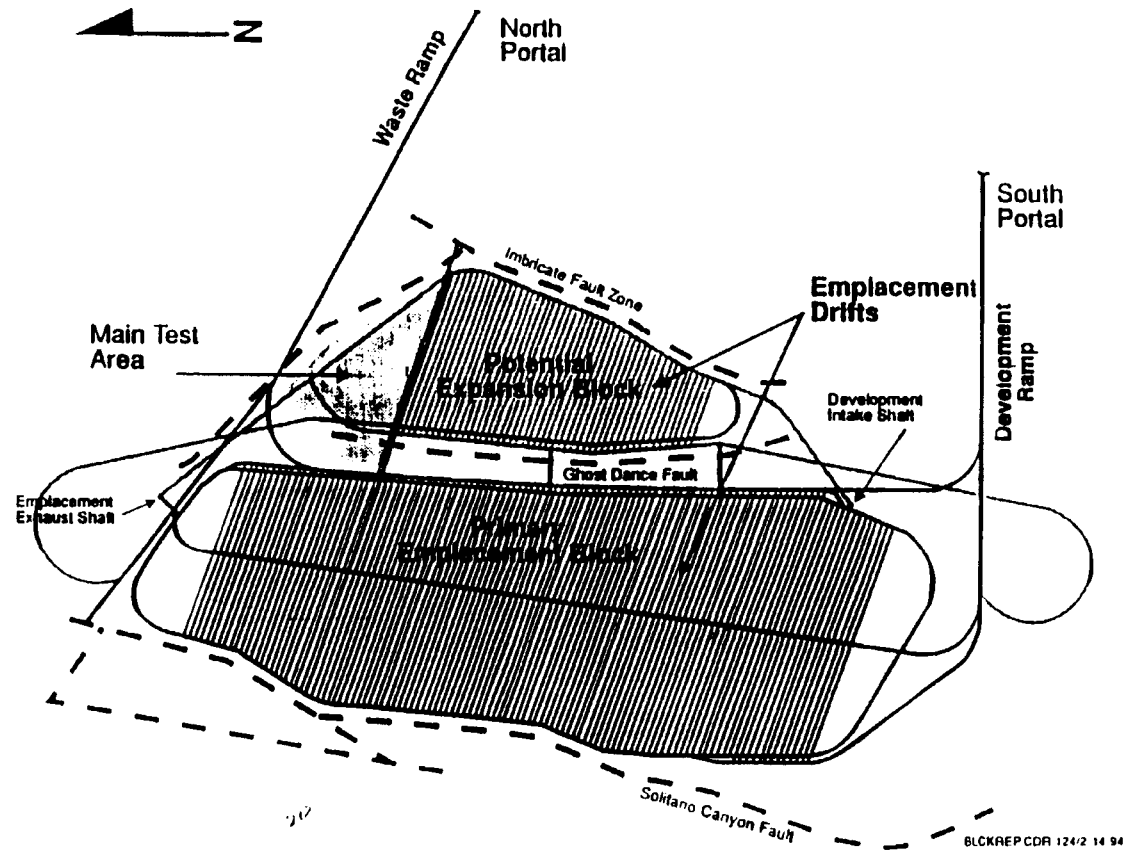


FIGURE 1. CONCEPTUAL REPOSITORY LAYOUT (DOE, 1994).

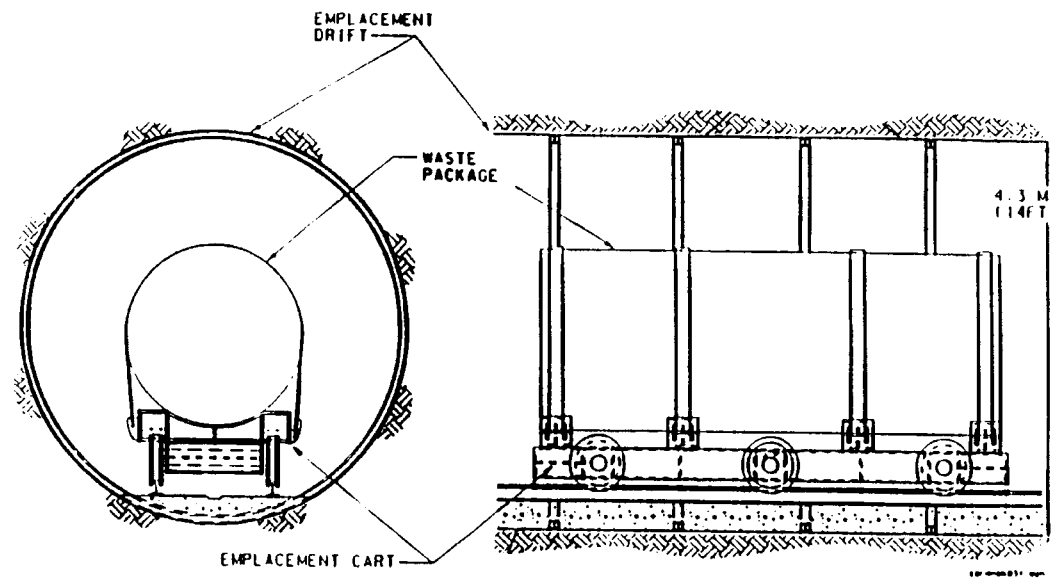


FIGURE 2. IN-DRIFT EMPLACEMENT CONCEPT (DOE, 1994).

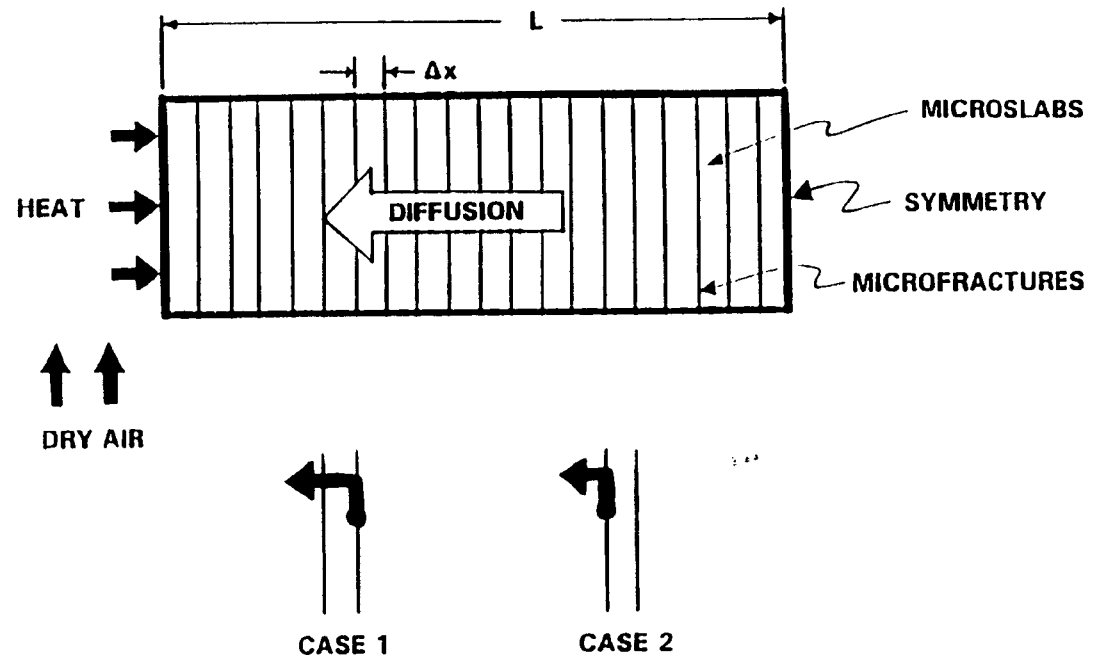


FIGURE 3. CONCEPTUAL 1D MODEL SHOWING CASES OF ASSUMED LIQUID VAPORIZATION.

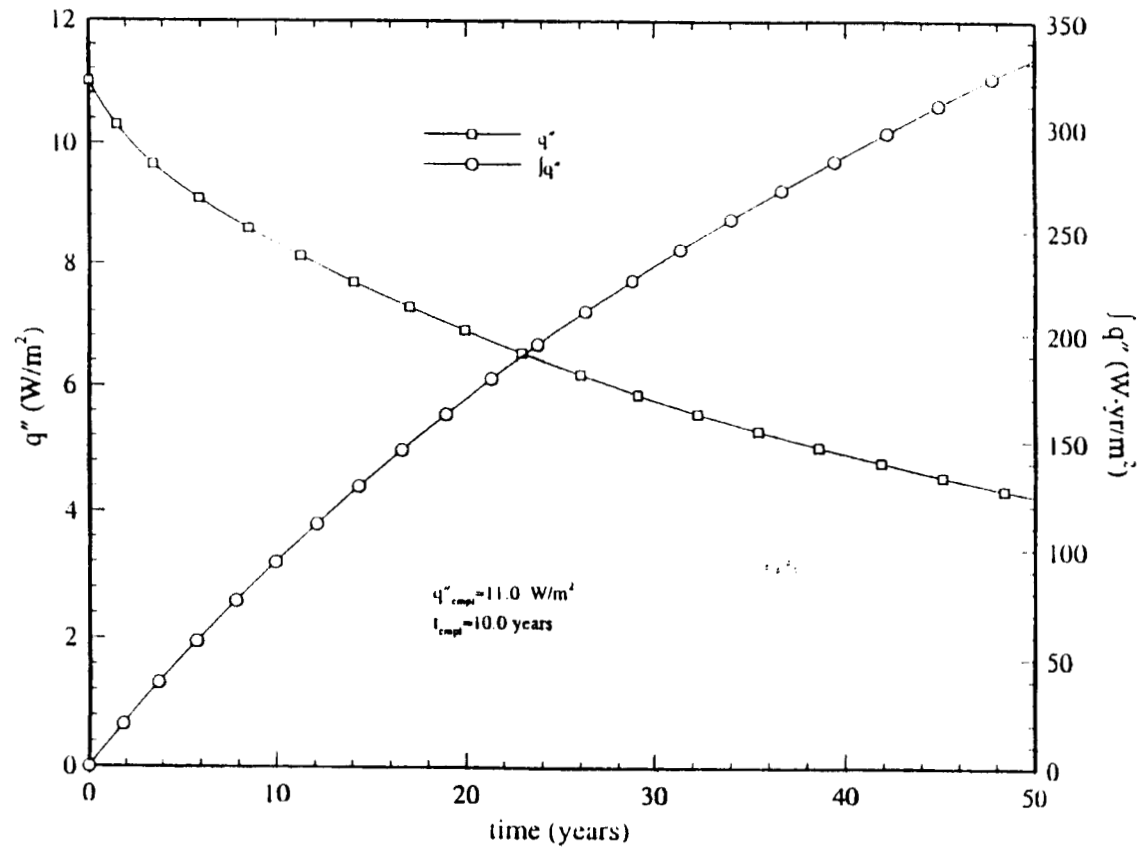


FIGURE 4. HEAT FLUX AND INTEGRATED HEAT FLUX USED IN CALCULATIONS.

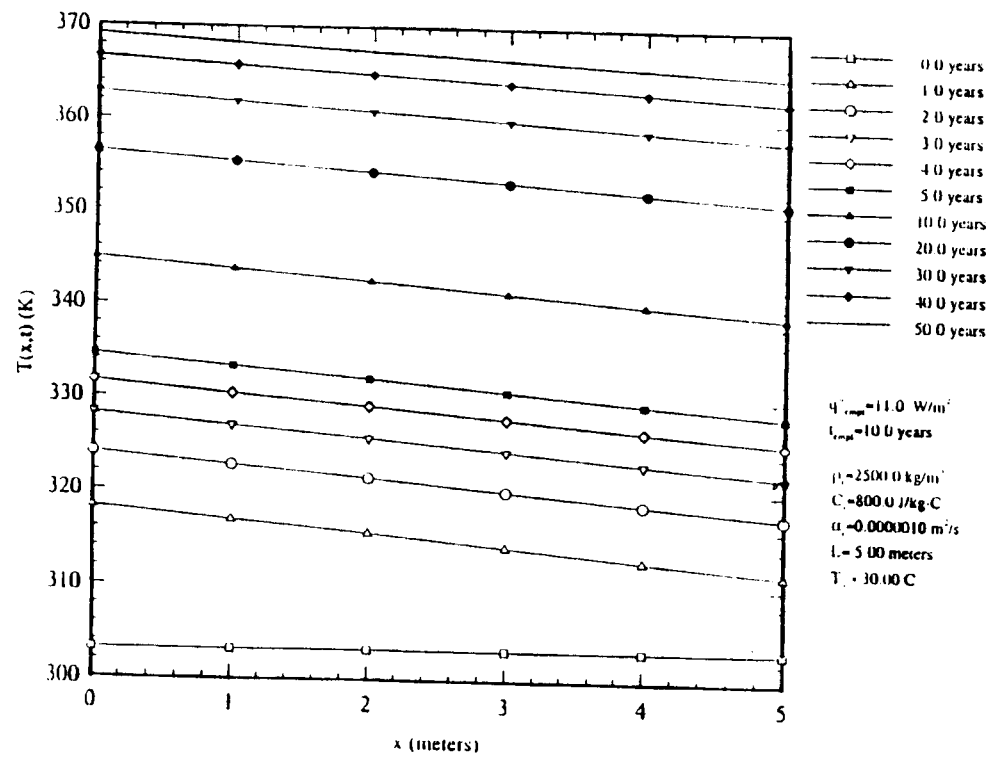


FIGURE 5. TEMPERATURE PROFILES.

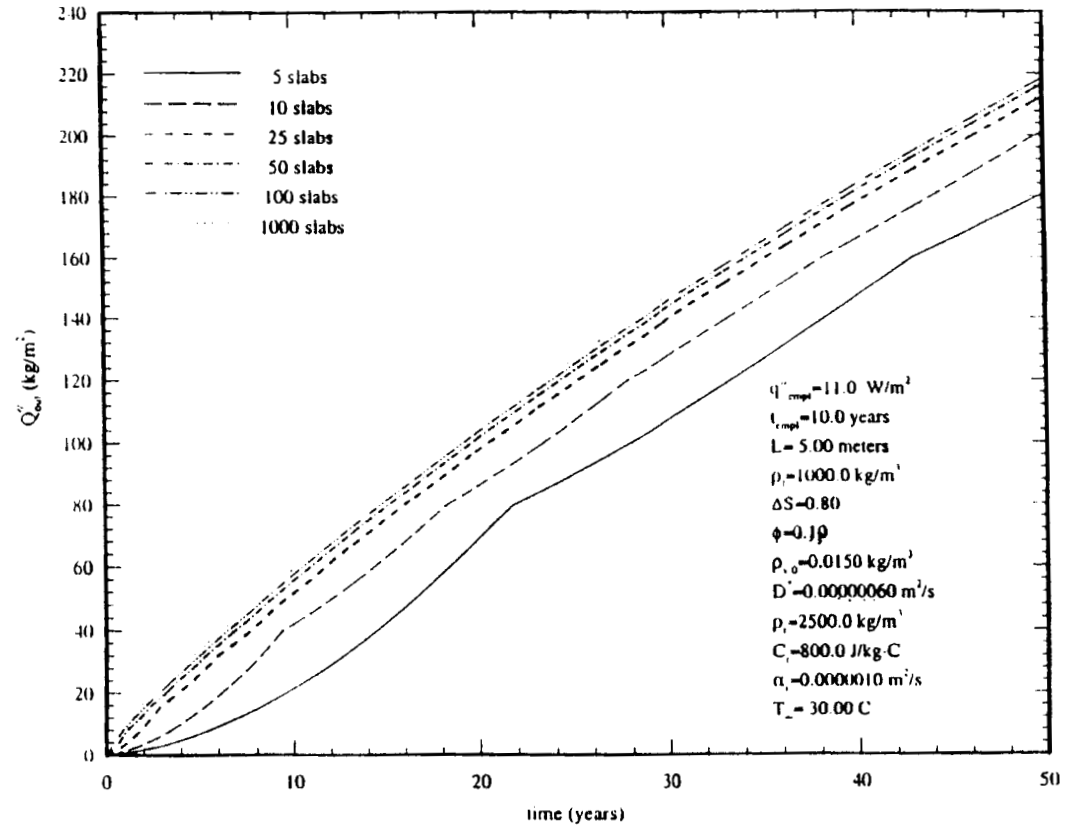


FIGURE 6. CUMULATIVE MASS OF LIQUID WATER REMOVED.

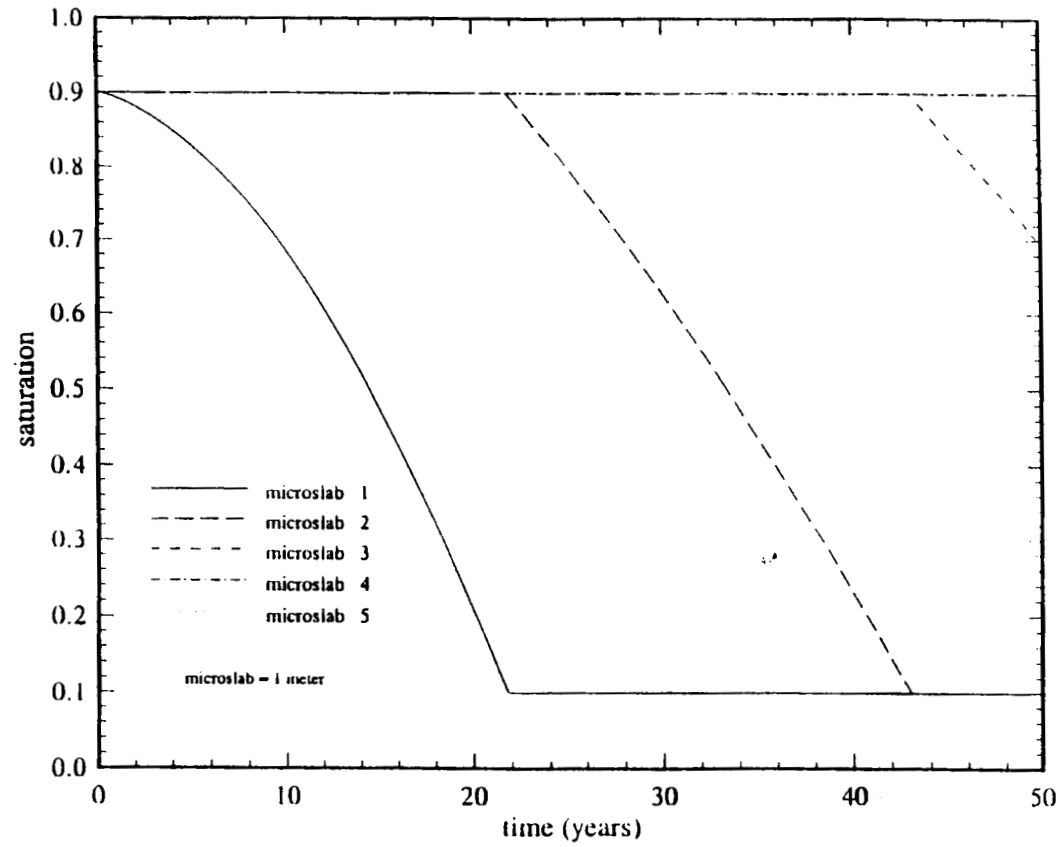


FIGURE 7. TRANSIENT SATURATION PROFILES FOR 5 MICROSLAB CASE.

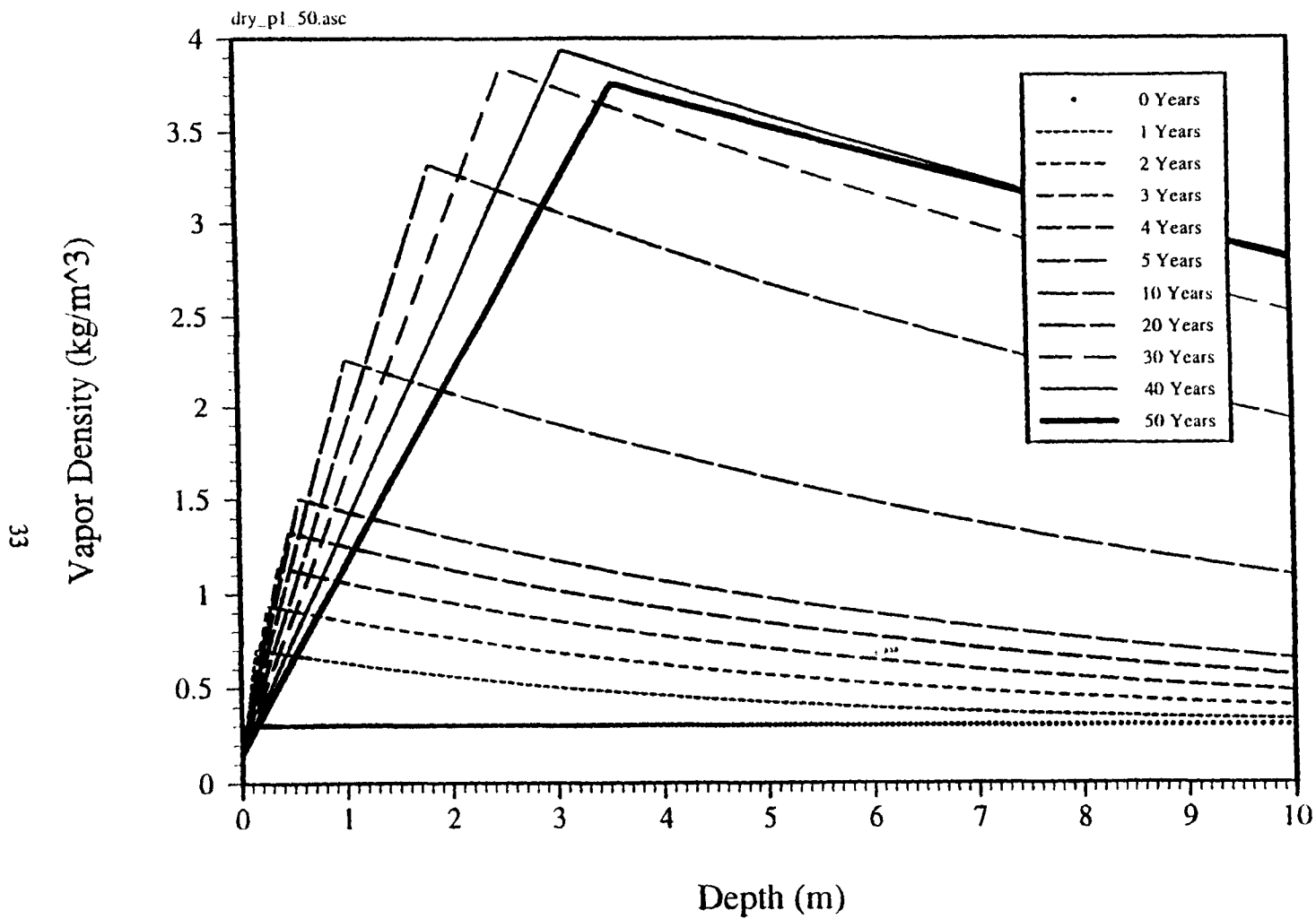


FIGURE 8a: VAPOR DENSITY PROFILES WITHOUT LIQUID ADVECTION (CALCULATED USING THE CODE BY STOTHOFF, 1994)

18/20

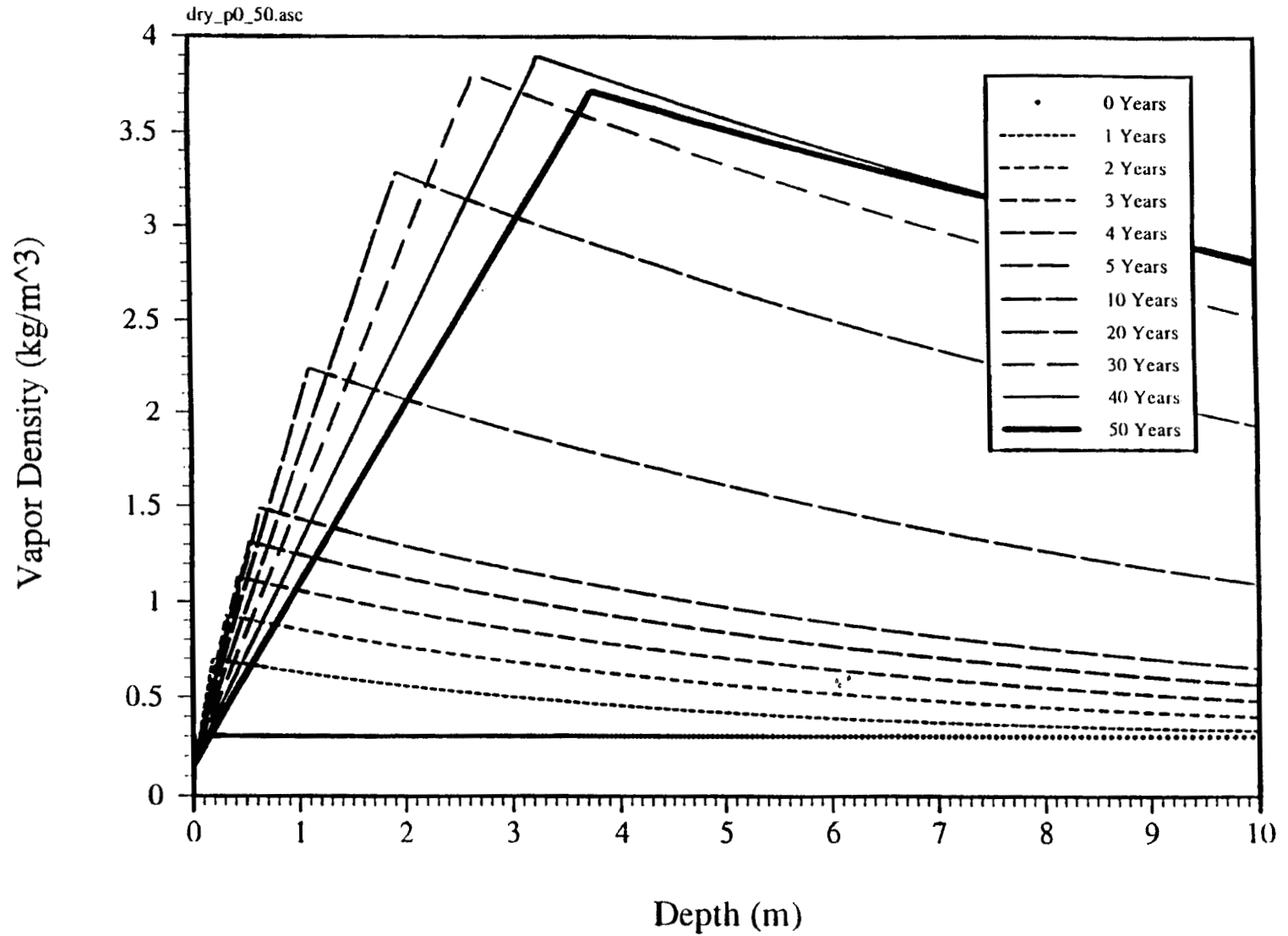


FIGURE 8b: VAPOR DENSITY PROFILES WITH LIQUID ADVECTION (CALCULATED USING THE CODE BY STOTHOFF, 1994)

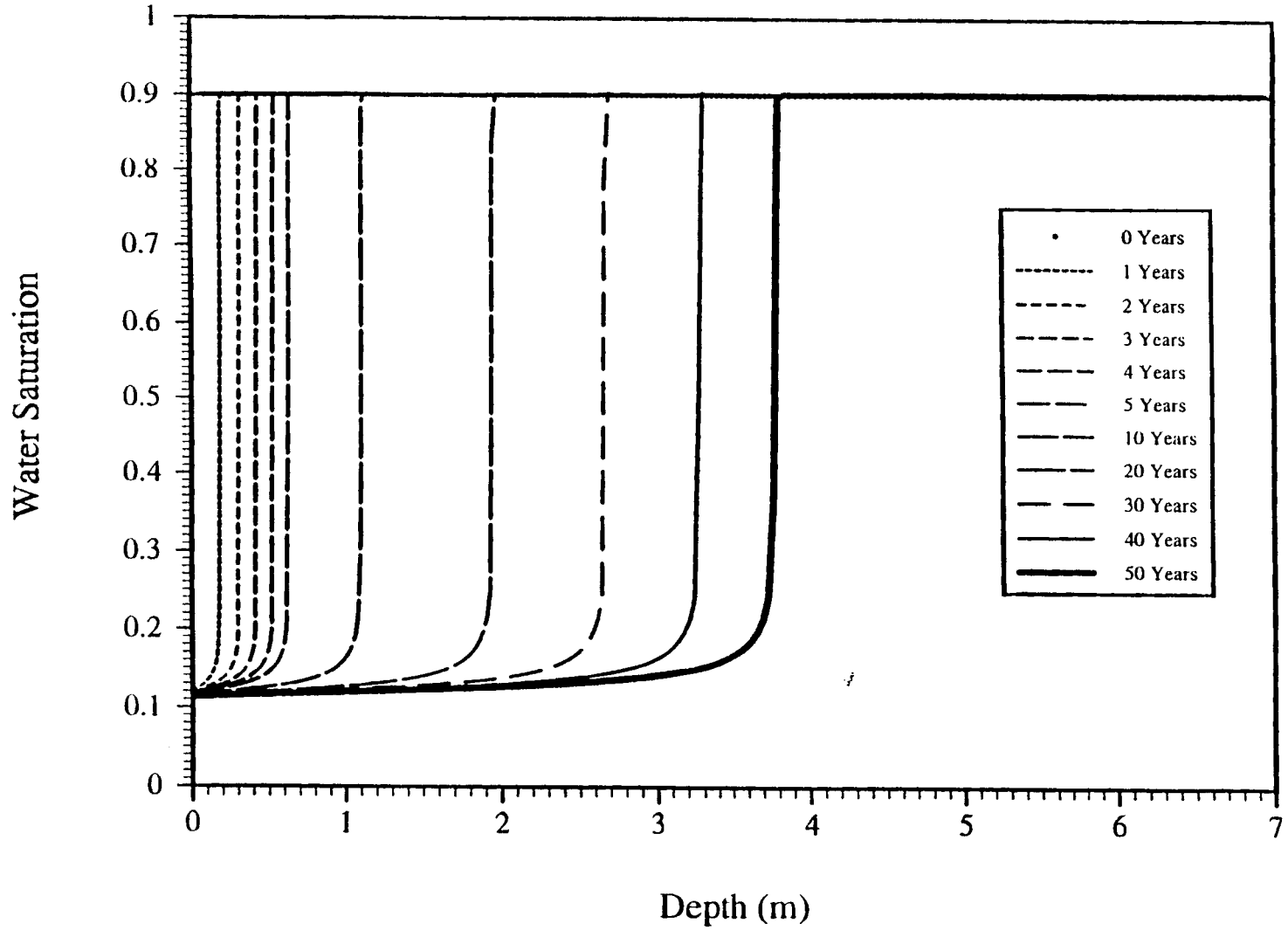


FIGURE 9a. LIQUID SATURATION PROFILES WITHOUT LIQUID ADVECTION (CALCULATED USING THE CODE BY STOTHOFF, 1994).

19/20

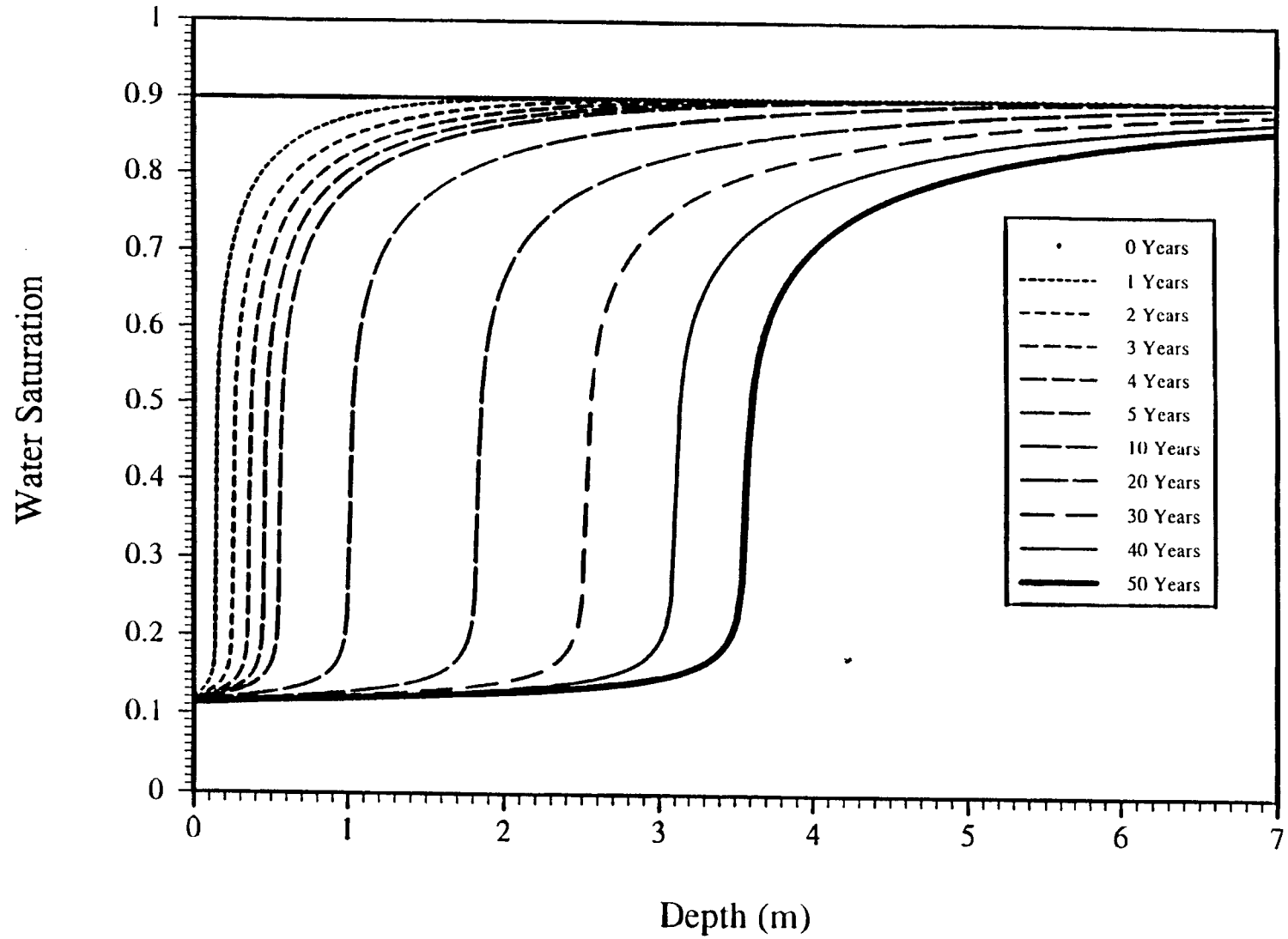


FIGURE 9b. LIQUID SATURATION PROFILES WITH LIQUID ADVECTION (CALCULATED USING THE CODE BY STOTHOFF, 1994).

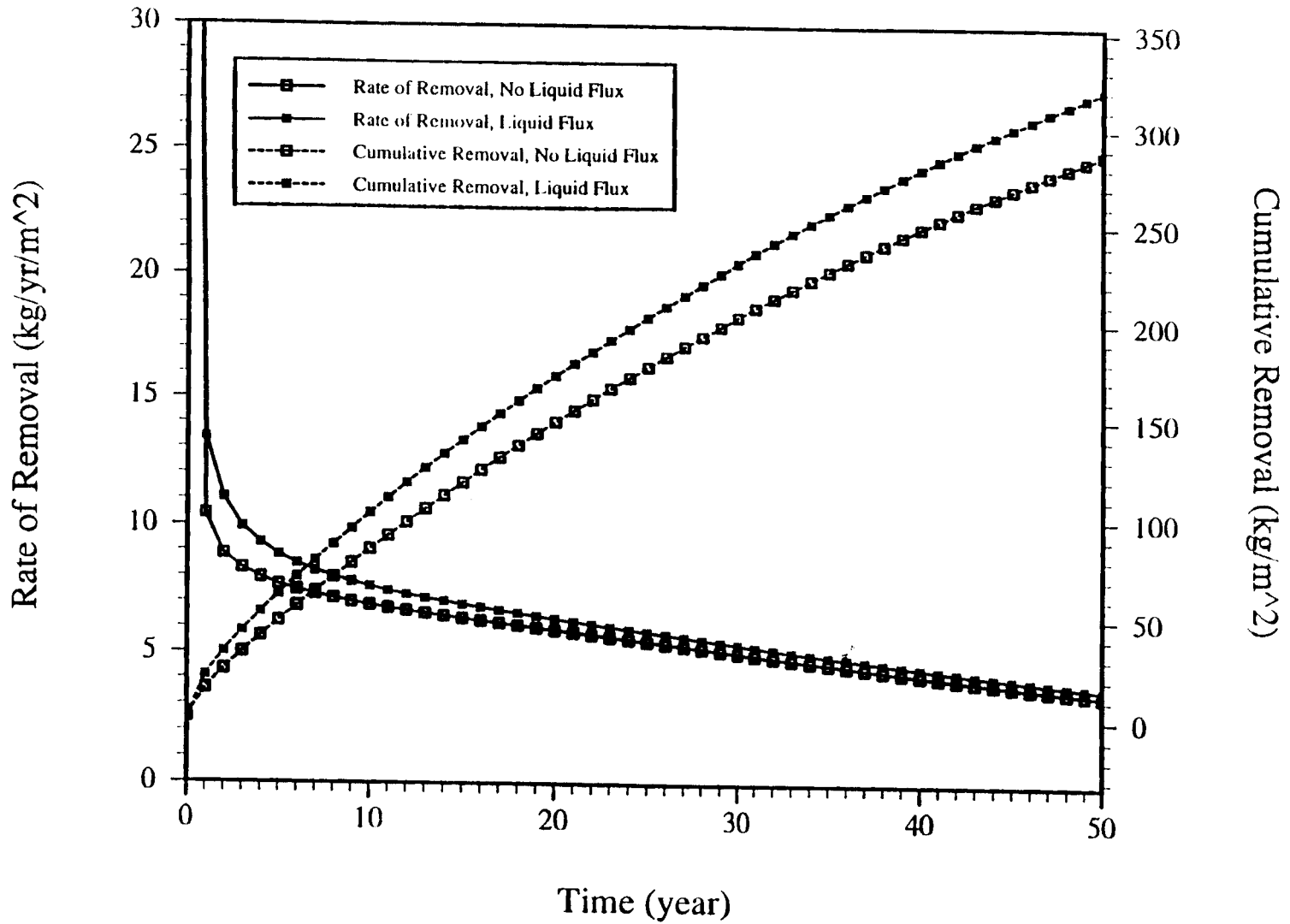


FIGURE 10. RATE OF REMOVAL AND CUMULATIVE REMOVAL OF LIQUID WATER (CALCULATED USING THE CODE BY STOTHOFF, 1994)

20/20